

The Twin Vortex Draft Tube Surge

Tony L. Wahl¹ Associate Member, Morris M. Skinner² Member,
Henry T. Falvey³ Member

Abstract

Recent studies conducted at Colorado State University using a model of the 700-MW turbines at the U. S. Bureau of Reclamation's Grand Coulee Third Powerplant indicate that in specific regions of the turbine hill curve a twin vortex draft tube surge exists. Extensive pressure fluctuation data were collected from transducers mounted at the draft tube throat, and dimensionless pressure and frequency parameters were calculated. The twin vortex produced pressure fluctuations at 2½-3 times the frequency typically associated with draft tube surging, and the pressure parameter was reduced in the twin vortex region. Evidence from the literature suggests that the twin vortex also occurs in other similar units.

Introduction

Draft tube surging in hydraulic reaction turbines has long been recognized as a phenomenon caused by excess swirl in the flow leaving the turbine runner under partial load or overload operating conditions. The investigations of Cassidy (1969), and Falvey and Cassidy (1970), established dimensionless pressure and frequency parameters for the pressure fluctuations due to the surge, and related these to a dimensionless swirl parameter, the length to diameter ratio of the draft tube, and the Reynolds number. The swirl parameter was computed from gross flow variables, and the behavior of the surge was assumed to be independent of the particular method used to introduce swirl.

$$\frac{f D_3^3}{Q} = \psi_1 \left(\frac{\Omega D_3}{\rho Q^2}, \frac{L}{D_3}, \frac{4Q}{\pi D_3 v} \right)$$

$$\frac{D_3^4 \sqrt{(p')^2}}{\rho Q^2} = \psi_2 \left(\frac{\Omega D_3}{\rho Q^2}, \frac{L}{D_3}, \frac{4Q}{\pi D_3 v} \right)$$

¹ Hydraulic Engineer, U. S. Bureau of Reclamation, P.O. Box 25007, Denver, Colorado, 80225.

² Associate Professor, Dept. of Civil Engineering, Colorado State University, Fort Collins, Colorado, 80523.

³ Consultant, P.O. Box 4, Conifer, Colorado, 80433.

where: ρ = density
 ν = kinematic viscosity
 D_3 = draft tube throat diameter
 L = draft tube length
 Q = discharge
 Ω = flux of angular momentum
 f = frequency of pressure fluctuation
 $\sqrt{(p')^2}$ = root-mean-square (rms) amplitude of pressure fluctuation
 $\left(\frac{f D_3^3}{Q}\right)$ = frequency parameter
 $\left(\frac{D_3^4 \sqrt{(p')^2}}{\rho Q^2}\right)$ = pressure parameter
 $\left(\frac{\Omega D_3}{\rho Q^2}\right)$ = draft tube swirl parameter
 $\left(\frac{4Q}{\pi D_3 \nu}\right)$ = Reynolds number

Initial investigations (Cassidy, 1969) in a wicket gate and draft tube model (no runner), using air as the working fluid, established that the frequency and pressure parameters are independent of viscous effects for Reynolds numbers above 80,000. The Reynolds number for prototype units and most hydraulic models is much greater than 80,000. Thus, for a given draft tube shape, the frequency and pressure parameters depend only on the swirl parameter.

The swirl parameter for the flow through the draft tube is calculated as the difference between the swirl introduced by the wicket gates and that extracted by the turbine runner. In a model having only wicket gates, the draft tube swirl parameter is constant for a given gate setting; each gate setting produces a different swirl parameter and corresponding surging behavior. However, in an operating turbine, each gate setting can produce a range of draft tube swirl parameters, and the same value of the draft tube swirl parameter can be obtained at different gate settings.

The primary objective of the tests described in this paper was to extend the research conducted previously on air models of draft tubes and wicket gate assemblies, by performing similar tests on an operating model turbine, in which the swirl parameter is affected by both wicket gate setting and turbine loading conditions. Additional details of these tests were documented by Wahl (1990).

Vortex Breakdown

The flow phenomenon associated with draft tube surging is described in the fluid mechanics literature as a vortex breakdown. Vortex breakdown may occur in unconfined flows, such as those over highly swept delta wings, or in confined flows, such as flows through draft tubes. Observations of the vortex breakdown in straight ducts have been provided by Harvey (1962) and Sarpkaya (1971). Cassidy and Falvey (1970), and Palde (1972) made similar observations for air flows through model draft tubes.

The most common flow structure associated with the vortex breakdown is a single helical vortex. However, Sarpkaya (1971), in experiments with a diverging tube, also observed a double vortex at low Reynolds numbers (1000 to 2000). The two spirals were intertwined together within the tube, 180° opposite one another. Escudier and Zehnder (1982) also observed the double vortex in straight, diverging tubes. The double vortex was unstable and intermittently reverted back to a single vortex.

Experimental Procedures

Test Facility

The model turbine used for these tests is a homologous, 1:40.3 scale model of the 700-MW turbines (units G22, G23, and G24) installed at the U. S. Bureau of Reclamation's (Reclamation's) Grand Coulee Third Powerplant. The test facility provides geometric similarity with the prototype installation from the penstock intake to the downstream tailrace. The model turbine was originally installed in the 1970's in a Reclamation test facility at Estes Powerplant in Colorado. The model was moved in 1988 to the Engineering Research Center at Colorado State University (CSU).

At CSU the model is installed in a once-through flow system drawing water directly from Horsetooth Reservoir, located immediately west of the laboratory. The model was originally designed to operate in the prototype head range of 220-355 ft (67.1-108.2 m). At the current installation, the maximum available head is about 250 ft (76.2 m). A butterfly valve and a 25-ft (7.62-m) standpipe downstream of the model are used to apply back pressure. Load is placed on the turbine by a water cooled, eddy current, absorption dynamometer. The dynamometer control console provides for both load and speed control of the unit.

The model draft tube is constructed of fiber glass, with a clear plastic throat section to allow observation of the flow. The model is equipped with air injection ports in the runner crown which were used for flow visualization at some test points. The operating status of the test facility and model turbine are monitored by a computerized data acquisition system collecting data from pressure transducers, thermocouples, a tachometer, and the dynamometer torque load cell.

Test Procedure

The model was operated at test points throughout the part-load surging region, with the frequency and amplitude of pressure fluctuations in the draft tube recorded for each test point. The head was maintained in the range 110-130 ft (33.5-39.6 m) for the majority of the tests; operation at desired points on the turbine hill curve was achieved by varying the runner speed at a given gate setting. The operating status of the turbine model was recorded for each test point using the data acquisition system. The vortex was made visible either by cavitation occurring in the vortex core or by admission of small quantities of air into the draft tube. To minimize the effects of cavitation all data were collected with tailwater levels set as high as possible; the cavitation index σ , was in the range 0.38-0.42 for most runs.

Pressure Fluctuation Measurements

Pressure surges in the draft tube were measured using two piezoresistive pressure transducers mounted at the draft tube throat, below the runner exit. The transducers were placed 180° apart, on the upstream side of the draft tube (location T1) and on the tailrace side (location T2), as shown in Figure 1.

The amplitude and frequency of pressure fluctuations at location T1 were recorded in the form of frequency spectra using a dynamic signal analyzer. AC coupling was used to record the fluctuation of pressure, rather than the absolute amplitude. An oscilloscope was used to monitor phase relationships between the signals.

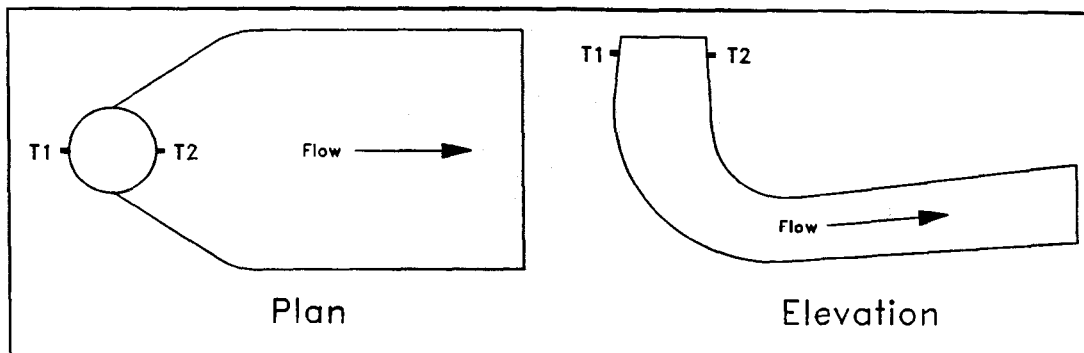


Figure 1. Schematic of pressure transducer locations on the elbow type draft tube.

Results and Analysis

Vortex Breakdown

The development of the draft tube surge in the model followed the well known sequence described in the literature. As the swirl was increased, the flow remained clear until a critical point at which vortex breakdown occurred suddenly, and a helical vortex developed in the draft tube in the form of a left-handed screw. The vortex precession was in the same direction as the runner rotation. The precession frequency of the vortex was about one-third to one-fourth of the rotational frequency of the runner, comparable to frequencies first reported by Rheingans (1937). Pressure fluctuations in the draft tube occurring at the precession frequency were asynchronous; the signals from locations T1 and T2 were approximately 180° out of phase with one another.

At gate settings above 19° (full gate setting for the prototype is 34°) the amplitude of pressure fluctuations and the size of the cavitating vortex core increased with increasing swirl. Also, the pitch of the vortex tended to increase as the swirl increased (i.e., the vortex became stretched out along the draft tube axis).

Twin Vortex

At gate settings less than 19°, cavitation of the vortex decreased as the swirl increased. The vortex was not visible at high tailwater levels, but could be seen at low tailwater levels. Injection of air into the draft tube at high tailwater produced only a cloud of bubbles in the flow. Despite the disappearance of a cavitating vortex, pressure fluctuations were still detected

in the draft tube at frequencies corresponding to the precession of a single helical vortex.

As the swirl approached 1.2, the dominant frequency of pressure fluctuations began to shift randomly between two different frequencies. The lower frequency corresponded to the precession of the single vortex observed previously. The higher frequency was generally 2½-3 times the lower frequency. The shifts occurred in a random manner, at intervals ranging from a few seconds to nearly a minute. As the swirl was increased further, the fluctuation became sustained at the higher frequency. When the tailwater was then lowered, two helical vortices could be seen in the draft tube, as shown in Figure 2. Each vortex retained the left-handed orientation of the original single vortex. While the twin vortex was present, the pressure fluctuations at locations T1 and T2 became in phase with one another. A sustained twin vortex was observed at a total of twelve test points, in the range of 9°-15° gate opening, and swirl values ranging from 1.2 to 3.0.

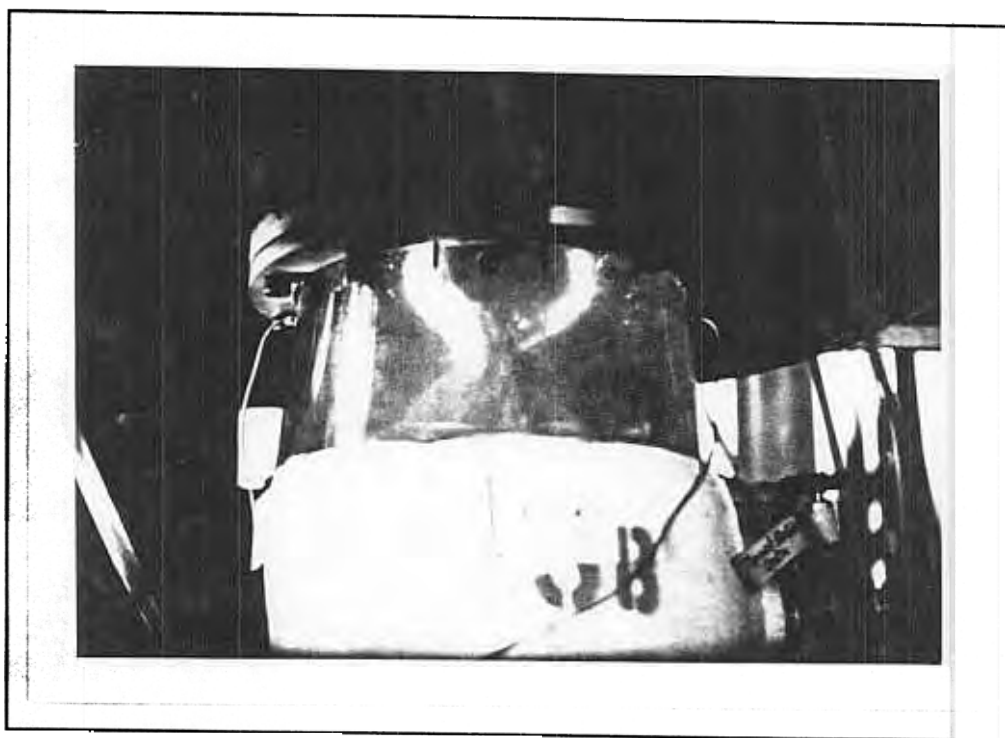


Figure 2. Photograph of twin vortex. The vortices are visible due to cavitation in the vortex cores. The exposure setting of the camera was matched to the strobe light frequency.

This behavior is similar to that noted by Fisher, Ulith, and Palde (1980) in a review of hydraulic model and prototype tests for the Grand Coulee Third, Marimbondo (Brazil), and Cerron Grande (Brazil) turbines. These installations have similar, but not homologous, turbines and elbow type draft tubes. In tests conducted on a 1:28 scale model of the 700-MW Grand Coulee Third turbines, a random shifting between two dominant frequencies was observed at about 46 percent of the best efficiency gate setting. The frequencies observed were similar to those seen in these tests. This behavior was also observed in model tests of the Marimbondo turbines at approximately the same gate setting. The

vortex was apparently not visible in either test.

Higher Frequency Surge

As the swirl was increased further at low gate openings, the twin vortex appeared to break down. The frequency of pressure fluctuations increased as the swirl increased, and it was no longer possible to make the vortex visible by either air injection or lowering of the tailwater. Near the limit of the operational range of the model, the dominant frequency was approximately equal to the runner rotational frequency. Data points in this region are marked as Region III in the figures that follow.

Frequency Parameter

Figure 3 shows the relationship of the frequency parameter to the swirl parameter. The figure clearly differentiates between the single and twin vortex conditions. At swirl values less than about 1.2, only the single vortex mode occurs. However, as the swirl increases above 1.2, the draft tube surge may consist of either a single or twin vortex.

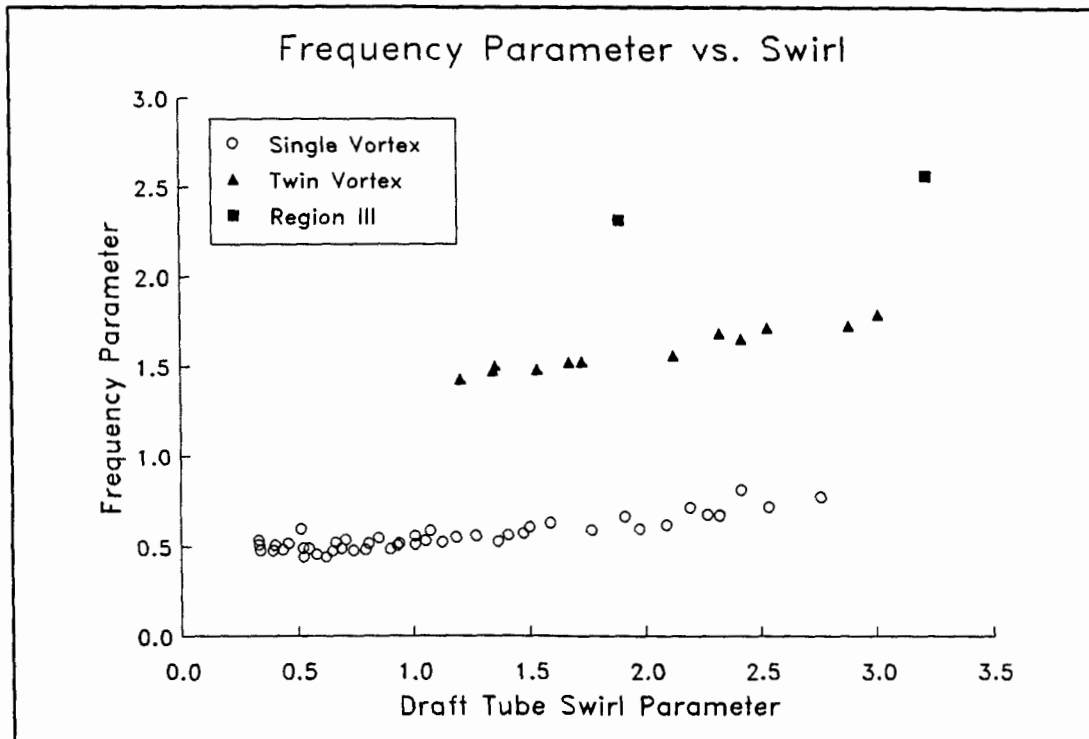


Figure 3. Frequency parameter vs. draft tube swirl parameter.

Pressure Parameter

A contour map of the pressure parameters for the dominant pressure fluctuation at each test point was constructed. The map was plotted on the speed ratio, ϕ_2 , and unit power, HP_{11} , axes defined as follows:

$$\phi_2 = \frac{\pi N D_2}{60 \sqrt{2gH}}$$

$$HP_{11} = \frac{(\text{bhp})}{D_2^2 H^{3/2}}$$

where: bhp = turbine output (brake horsepower)
 D_2 = throat diameter of turbine runner, ft
 H = net head, ft
 N = runner speed, rpm

Figure 4 shows two peaks in the pressure parameter, separated by a low saddle. The saddle region corresponds roughly with the region in which the twin vortex was observed.

Figure 5 shows the pressure parameter values plotted against the swirl parameter. Points where a twin vortex was observed are marked on the plot. Figure 6 shows the same data divided between small gate openings (less than 50 percent) and large gate openings (greater than 50 percent). The pressure parameter correlates well with the swirl parameter at the large gate settings. However, in the lower range of gate settings, the pressure parameter varies widely. The behavior of the pressure parameter in this range is better explained by the pressure parameter map (Figure 4).

Conclusions

Prior research has indicated that for a given draft tube shape, operating at suitably high Reynolds numbers, the amplitude and frequency of draft tube surge pressure fluctuations depend only on the value of the draft tube swirl parameter. However, these tests have indicated that in some cases the draft tube swirl parameter does not fully explain the behavior of the draft tube surge over the complete operating range of a turbine, due to the existence of two possible surging modes. The following conclusions can be drawn:

- * A twin vortex draft tube surge was observed in a well defined region of the model turbine hill curve. Evidence in the literature suggests that this surging mode may also occur in other similar models and prototype units.
- * The frequency parameter is dependent not only on the draft tube swirl parameter, but also on the number of helical vortices in the draft tube. In this model at swirl parameter values above 1.2, the frequency parameter becomes a multivalued function of the swirl, depending on whether the flow contains a single or twin vortex.
- * The transition from the single to the twin vortex is unstable. In the transition zone, either form may exist, and the flow in the draft tube seems to alternate randomly between the two modes.
- * The pressure parameter is related to the swirl parameter only at high wicket gate settings (above about one-half of the full gate opening). At low gate settings, there is little relationship between the pressure parameter and the swirl parameter; the behavior of the pressure parameter was better explained by the pressure parameter map.
- * The pressure fluctuations associated with the twin vortex are well above the Rheingans frequency generally associated with draft tube surging. The increase in frequency due to the formation of the twin vortex is due not only to a doubling of the number of vortices, but also to an increase in the vortex precession frequency.

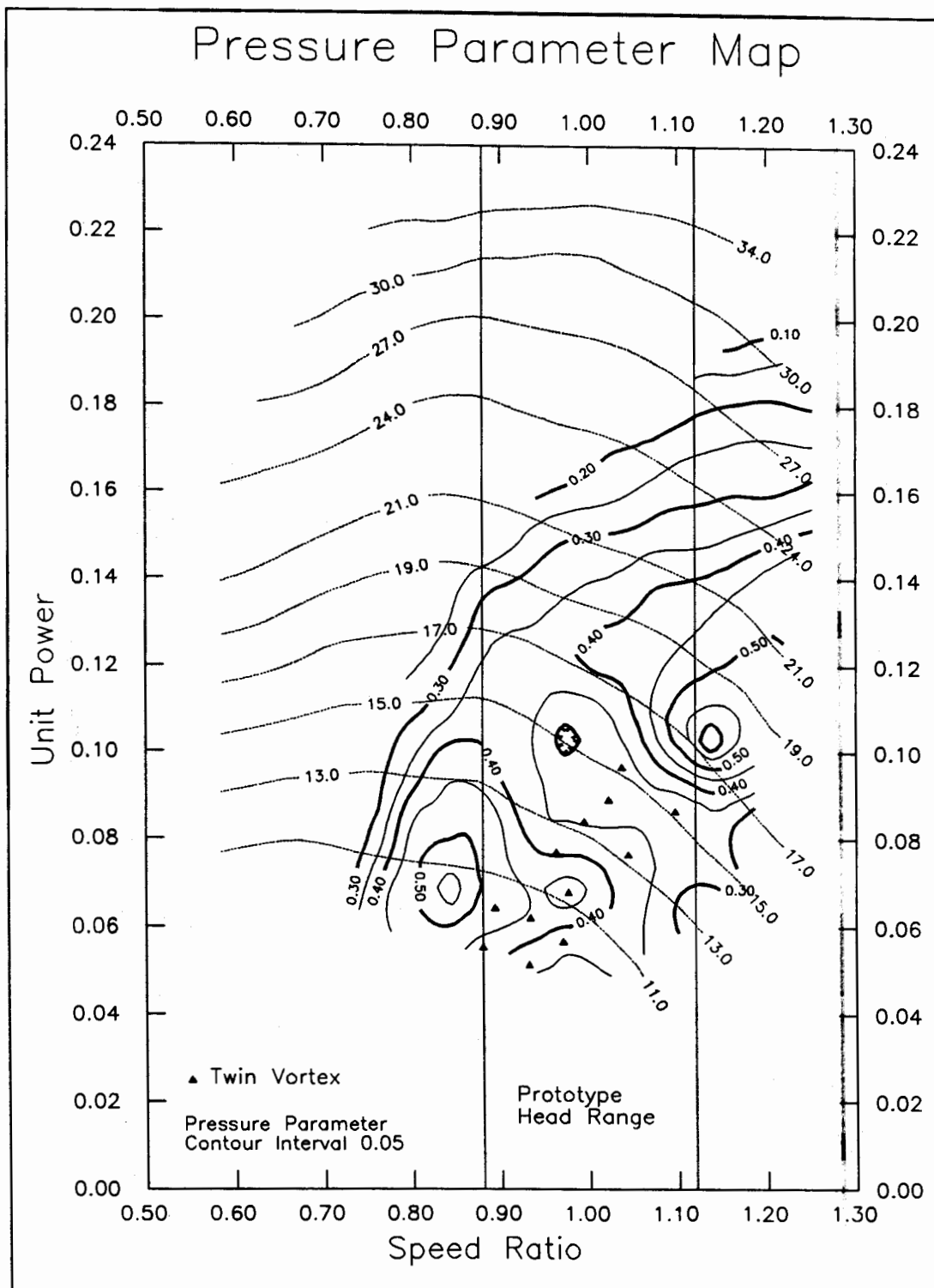


Figure 4. Pressure parameter map. Solid triangles indicate a sustained twin vortex. Dotted lines are labeled with wicket gate setting in degrees. The unit power HP_{11} is given in units of $\text{hp}/\text{ft}^{3.5}$. The speed ratio ϕ_2 is dimensionless.

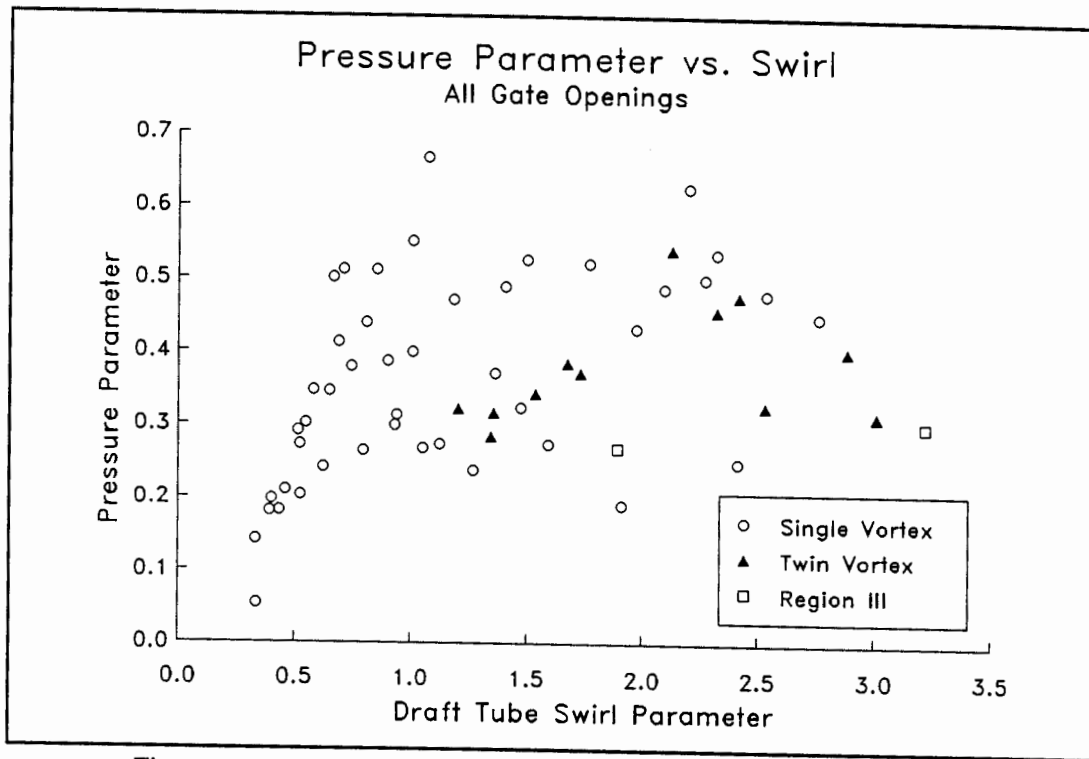


Figure 5. Pressure parameter vs. swirl for all gate settings.

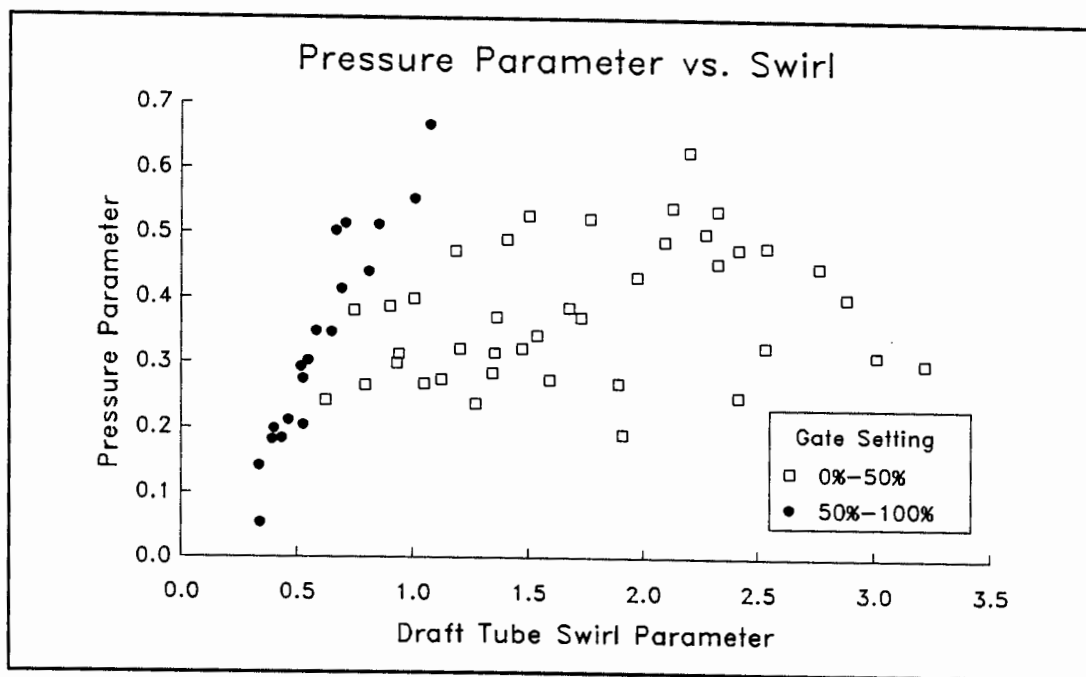


Figure 6. Pressure parameter vs. swirl by gate setting.

Acknowledgments

This study was funded by the Department of Civil Engineering at Colorado State University, Fort Collins, Colorado.

SI Units

Values of unit power (HP_{11} , $hp/ft^{3.5}$) shown on Figure 4 may be converted to the SI equivalent (P_{11} , $kW/m^{3.5}$), by the following equation:

$$P_{11} = 47.7 HP_{11}$$

References

- Cassidy, J. J., "Experimental Study and Analysis of Draft Tube Surging," *REC-OCE-69-5, Report No. Hyd-591*, U. S. Bureau of Reclamation, Oct. 1969.
- Cassidy, J. J., and H. T. Falvey, "Observations of Unsteady Flow Arising After Vortex Breakdown," *Journal of Fluid Mechanics*, Vol. 41, 1970, pp. 727-736.
- Escudier, M. P., and N. Zehnder, "Vortex Flow Regimes," *Journal of Fluid Mechanics*, Vol. 115, 1982, pp. 105-121.
- Falvey, H. T., and J. J. Cassidy, "Frequency and Amplitude of Pressure Surges Generated by Swirling Flow," *Proceedings*, 5th Symposium IAHR/AIRH Section for Hydraulic Machinery Equipment and Cavitation, Stockholm, Sweden, 1970.
- Fisher, R. K., Jr., U. J. Palde, and P. Ulith, "Comparison of Draft Tube Surging of Homologous Scale Models and Prototype Francis Turbines," *Proceedings*, 10th Symposium IAHR/AIRH Section for Hydraulic Machinery Equipment and Cavitation, Tokyo, Japan, 1980.
- Harvey, J. K., "Some Observations of the Vortex Breakdown Phenomenon," *Journal of Fluid Mechanics*, Vol. 14, 1962, pp. 585-592.
- Palde, U. J., "Influence of Draft Tube Shape on Surging Characteristics of Reaction Turbines," *Report No. REC-ERC-72-24*, U. S. Bureau of Reclamation, July 1972.
- Rheingans, W. J., "Power Swings in Hydroelectric Power Plants," *Transactions of the ASME*, Vol. 62, No. 174, Apr. 1940, pp. 171-184.
- Sarpkaya, T., "On Stationary and Travelling Vortex Breakdowns," *Journal of Fluid Mechanics*, Vol. 45, 1971, pp. 545-559.
- Wahl, T. L., "Draft Tube Surging Hydraulic Model Study," *Thesis*, in partial fulfillment of the requirements for the degree of Master of Science, Colorado State University, Summer 1990.

List of Keywords

cavitation
draft tube
hydraulic models
vortex
swirl
turbines
hydroelectric power generation
powerplants